PHYSICAL REVIEW D **79,** 074019 (2009)

Effects of unparticles on top spin correlation at the Large Hadron Collider

Masato Arai,[1,*] Nobuchika Okada,[2,†] and Karel Smolek[3,‡]

[1]*Center for Quantum Spacetime (CQUeST), Sogang University, Shinsu-dong 1, Mapo-gu, Seoul 121-742, Korea*

[2]*Theory Group, KEK, Tsukuba, 305-0801, Japan*

[3]*Institute of Experimental and Applied Physics, Czech Technical University in Prague, Horská 3a/22, 128 00 Prague 2, Czech Republic*

(Received 6 February 2009; published 21 April 2009)

We study effects of the scale-invariant hidden sector, the unparticle, proposed by Georgi, on top spin correlation at the Large Hadron Collider. Assuming no flavor-changing interaction between the unparticles and the standard model particles, the top-antitop quark pair production process arises through virtual unparticle exchanges in the s channel, in addition to the standard model processes. In particular, we consider contributions of scalar and vector unparticles and find that these make sizable deviations of the top spin correlation from the standard model one.

DOI: 10.1103/PhysRevD.79.074019 PACS numbers: 14.65.Ha

I. INTRODUCTION

The standard model (SM) quite successfully describes phenomena around the electroweak scale. However, it is widely believed that new physics beyond the SM appears around the TeV scale or higher. Recently, Georgi proposed a conceptually new possibility that scale-invariant new physics with an infrared fixed point couples to the SM sector [1,2], based on a specific model possessing the scale invariance [3]. Interactions between the new physics sector and the SM sector are realized in the following way. First we introduce couplings between the new physics operator $\mathcal{O}_{\rm UV}$ with mass dimension $d_{\rm UV}$, which is a singlet under the SM gauge group, and the SM operator $\mathcal{O}_{\rm SM}$ with mass dimension $d_{\rm SM}$ at a mass scale M,

$$\mathcal{L}_{\rm int} = \frac{c_n}{M^{d_{\rm UV}+d_{\rm SM}-4}}\mathcal{O}_{\rm UV}\mathcal{O}_{\rm SM}, \tag{1.1}$$

where c_n is a dimensionless constant. It is assumed that the new physics sector has an infrared fixed point at a scale $\Lambda_{\rm UV}$, below which the operator $\mathcal{O}_{\rm UV}$ matches onto a new (composite) operator $\mathcal{O}_{\mathcal{U}}$ with dimension $d_{\mathcal{U}}$ through the dimensional transmutation. As a result, an effective interaction term arises of the form

$$\mathcal{L}_{\rm int} = c_n\frac{\Lambda_{\rm UV}^{d_{\rm UV}-d_{\mathcal{U}}}}{M^{d_{\rm UV}+d_{\rm SM}-4}}\mathcal{O}_{\mathcal{U}}\mathcal{O}_{\rm SM} \equiv \frac{\lambda_n}{\Lambda^{d_{\mathcal{U}}+d_{\rm SM}-4}}\mathcal{O}_{\mathcal{U}}\mathcal{O}_{\rm SM}, \tag{1.2}$$

where λ_n is a coupling constant and Λ is an effective cutoff scale of low energy physics. The operator $\mathcal{O}_{\mathcal{U}}$ is coined an unparticle. Depending on the nature of the new physics operator $\mathcal{O}_{\rm UV}$, the resulting unparticle may have a different Lorentz structure. Three unparticle operators, the Lorentz scalar $\mathcal{O}_{\mathcal{U}}$, the vector $\mathcal{O}^{\mu}_{\mathcal{U}}$, and the tensor $\mathcal{O}^{\mu\nu}_{\mathcal{U}}$, were considered [1], and their two-point functions were derived from the argument based on scale invariance [2,4]. By using these operators, new phenomena such as direct unparticle emission processes [1] and virtual unparticle exchange processes [2,4] were also discussed. In particular, virtual unparticle exchange processes are interesting since unparticles with a possible different spin nature affect the spin configuration and angular distribution of outgoing SM particles.

Suitable candidates to produce the effects of virtual unparticle exchange are top spin correlations in the top-antitop pair production process. The top quark with a mass range of 175 GeV [5] decays electroweakly before hadronizing [6], and thus the information of polarization of the top-antitop quark pair is directly transferred to its decay products without being diluted by hadronization. The spin correlations for the hadronic top-antitop pair production process have been extensively studied in QCD [7–9]. It is then found that there is a spin asymmetry between the top-antitop pairs produced; namely, the number of top-antitop quark pairs produced with both spin up or spin down (like pairs) is different from the number of pairs with the opposite spin combinations (unlike pairs). If the top quark is coupled to new physics beyond the SM, new physics effects could alter the top-antitop spin correlations. Therefore, the top-antitop spin correlations can provide useful information to test not only the SM, but also possible new physics. Effects of new physics on the top-antitop spin correlations have been studied at e^+e^- [10] and photon [11] colliders. It should be noticed that the LHC is a promising laboratory to study the top-antitop quark production and the top spin correlations, since it will produce almost 10×10^6 top quarks a year. Effects of several new physics models, such as Kaluza-Klein gravitons in brane-world models [12,13] and Z' bosons [14] on top spin correlations at the LHC, were studied, and sizable deviations of the top spin correlations from the SM ones were found. Also, analysis of top spin correlations through

*arai@sogang.ac.kr
†okadan@post.kek.jp
‡karel.smolek@utef.cvut.cz

 © 2009 The American Physical Society

possible new physics has been performed in a model-independent way with the use of Monte Carlo simulation [15].

So far, there have been some studies on the effects of unparticles on top-antitop quark pair production processes. The total cross section of top-antitop quark pair production through virtual unparticle exchanges was studied at hadron colliders [16], the International Linear Collider (ILC) [17], and photon colliders [18]. For the ILC and photon colliders, the top spin correlation was also studied [19,20]. In this paper we investigate the effects of scalar and vector unparticles on the top-antitop pair production and its spin correlations at the LHC. In addition to the SM processes, the unparticle gives rise to a new contribution for the top-antitop pair production process in the s channel through the effective coupling (1.2) and alters the top-antitop pair production cross section and the top spin correlations from the SM ones.

This paper is organized as follows. In the next section, we briefly review the top spin correlations. In Sec. III, we give a short discussion on the basics of unparticle physics. In Sec. IV, we derive the invariant amplitudes for the polarized top-antitop pair production processes mediated by the scalar and vector unparticles. We show the results of our numerical analysis in Sec. V. Section VI is devoted to conclusions. The Appendix contains the formulas used in our calculations.

II. TOP SPIN CORRELATION

At hadron colliders, the top-antitop quark pair is produced through the processes of quark-antiquark pair annihilation and gluon fusion:

$$i \to t + \bar{t}, \qquad i = q\bar{q}, gg. \tag{2.1}$$

The former is the dominant process at the Tevatron, while the latter is dominant at the LHC. The produced top-antitop pairs decay before hadronization takes place. The main decay modes in the SM involve leptonic and hadronic modes:

$$t \to bW^+ \to bl^+\nu_l, bu\bar{d}, bc\bar{s}, \tag{2.2}$$

where $l = e, \mu, \tau$. The differential rates of decay to a decay product $f = b, l^+, \nu_l$, etc. at the top quark rest frame can be parametrized as

$$\frac{1}{\Gamma}\frac{d\Gamma}{d\cos\theta_f} = \frac{1}{2}(1 + \kappa_f \cos\theta_f), \tag{2.3}$$

where Γ is the partial decay width of the respective decay channel and θ_f is the angle between the top quark polarization and the direction of motion of the decay product f. The coefficient κ_f, which is called the top spin analyzing power, is a constant between -1 and 1. The ability to distinguish the polarization of the top quark evidently increases with κ_f. The most powerful spin analyzer is a charged lepton, for which $\kappa_{l^+} = +1$ at tree level [21]. Other values of κ_f are $\kappa_b = -0.41$ for the b quark and $\kappa_{\nu_l} = -0.31$ for the ν_l, respectively. In hadronic decay modes, the role of the charged lepton is replaced by the $\bar{d}$ or $\bar{s}$ quark.

Now we see how top spin correlations appear in the chain of processes of $i \to t\bar{t}$ and decay of the top quarks. The total matrix element squared for the top-antitop pair production (2.1) and its decay channels (2.2) is given by

$$|\mathcal{M}|^2 \propto \mathrm{Tr}[\rho R^i \bar{\rho}] = \rho_{\alpha'\alpha} R^i_{\alpha\beta,\alpha'\beta'} \bar{\rho}_{\beta'\beta} \tag{2.4}$$

in the narrow-width approximation for the top quark. Here the subscripts denote the top and antitop spin indices, and R^i denotes the density matrix corresponding to the production of the on-shell top-antitop quark pair through the process i in (2.1):

$$R^i_{\alpha\beta,\alpha'\beta'} = \sum_{\text{initial spin}} \mathcal{M}(i \to t_\alpha \bar{t}_\beta)\mathcal{M}^*(i \to t_{\alpha'}\bar{t}_{\beta'}), \tag{2.5}$$

where $\mathcal{M}(i \to t_\alpha \bar{t}_\beta)$ is the amplitude for the top-antitop pair production. The matrices ρ and $\bar{\rho}$ are the density matrices corresponding to the decays of polarized top and antitop quarks into some final states at the top and antitop rest frames, respectively. In the leptonic decay modes, the matrices ρ, which lead to (2.3), can be obtained as (see, for instance, [22])

$$\begin{aligned}\rho_{\alpha'\alpha} &= \mathcal{M}(t_\alpha \to bl^+\nu_l)\mathcal{M}^*(t_{\alpha'} \to bl^+\nu_l) \\ &= \frac{\Gamma}{2}(1 + \kappa_f \vec{\sigma}\cdot\vec{q}_f)_{\alpha'\alpha},\end{aligned} \tag{2.6}$$

where q_f is the unit vector of the direction of motion of the decay product f. The density matrix for the polarized antitop quark is obtained by replacing $\kappa_f \to -\kappa_f$ in (2.6) if there is no CP violation. In the SM, there is no CP violation in the top quark decay at leading order. In the model presented in the next section, there is no contribution that breaks CP symmetry at leading order, and thus this relation holds.

A way to analyze the top-antitop spin correlations is to see the angular correlations of two charged leptons l^+l^- produced by the top-antitop quark leptonic decays. In the following, we consider only the leptonic decay channels. Using (2.4), (2.5), and (2.6) and integrating over the azimuthal angles of the charged leptons, we obtain the following double distribution [7,8]:

$$\begin{aligned}\frac{1}{\sigma}\frac{d^2\sigma}{d\cos\theta_{l^+}d\cos\theta_{l^-}} = \frac{1}{4}(1 &+ B_1\cos\theta_{l^+} + B_2\cos\theta_{l^-} \\ &- C\cos\theta_{l^+}\cos\theta_{l^-}).\end{aligned} \tag{2.7}$$

Here σ denotes the cross section for the process of the leptonic decay modes, and $\theta_{l^+}(\theta_{l^-})$ denotes the angle between the top (antitop) spin axis and the direction of motion of the antilepton (lepton) at the top (antitop) rest

frame. In what follows, we use the helicity spin basis, which is an almost optimal basis to analyze the top spin correlation at the LHC.[1] In this basis, the top (antitop) spin axis is regarded as the direction of motion of the top (antitop) in the top-antitop center-of-mass system. The coefficients B_1 and B_2 are associated with a polarization of the top and antitop quarks, and C encodes the top spin correlations, whose explicit expression is given by

$$C = \mathcal{A}\kappa_{l^+}\kappa_{l^-}, \qquad \kappa_{l^+} = \kappa_{l^-} = 1, \tag{2.8}$$

where the coefficient $\mathcal{A}$ represents the spin asymmetry between the top-antitop pairs produced with like- and unlike-spin pairs and is defined as

$$\mathcal{A} = \frac{\sigma(t_\uparrow\bar{t}_\uparrow) + \sigma(t_\downarrow\bar{t}_\downarrow) - \sigma(t_\uparrow\bar{t}_\downarrow) - \sigma(t_\downarrow\bar{t}_\uparrow)}{\sigma(t_\uparrow\bar{t}_\uparrow) + \sigma(t_\downarrow\bar{t}_\downarrow) + \sigma(t_\uparrow\bar{t}_\downarrow) + \sigma(t_\downarrow\bar{t}_\uparrow)}. \tag{2.9}$$

Here $\sigma(t_\alpha\bar{t}_\beta)$ is the cross section of the top-antitop pair production at parton level with denoted spin indices.

In the SM, at the lowest order of α_s, the spin asymmetry is found to be $\mathcal{A} = +0.319$ for the LHC.[2] In the ATLAS experiment at the LHC, the spin asymmetry of the top-antitop pairs will be measured with a precision of several percent, after one year at low luminosity (10 fb^{-1}) [25]. This accuracy can enhance the feasibility of finding new physics effects at the LHC through top spin correlation.

III. UNPARTICLE PHYSICS

We briefly review derivations of two-point functions of scalar and vector unparticles, which are relevant for our analysis. It was argued in [2] that the scale invariance can be used to fix the two-point function of unparticle operators,

$$\langle 0|\mathcal{O}_\mathcal{U}(x)\mathcal{O}^\dagger_\mathcal{U}(0)|0\rangle = \int \frac{d^4P}{(2\pi)^2} e^{-iP\cdot x}\rho(P^2), \tag{3.1}$$

where $\rho(P^2) = (2\pi)^2 \int d\lambda \delta^4(P - p_\lambda)|\langle 0|\mathcal{O}_\mathcal{U}|\lambda\rangle|^2$. The spectral function $\rho(P^2)$ is determined by scale invariance to be $\rho(P^2) = A_{d_\mathcal{U}}\theta(P^0)\theta(P^2)(P^2)^{d_\mathcal{U}-2}$, where $A_{d_\mathcal{U}}$ is the normalization factor. This factor is fixed, by identifying $\rho(P^2)$ with $d_\mathcal{U}$-body phase space of massless particles, to be

$$A_{d_\mathcal{U}} = \frac{16\pi^2\sqrt{\pi}}{(2\pi)^{2d_\mathcal{U}}} \frac{\Gamma(d_\mathcal{U} + 1/2)}{\Gamma(d_\mathcal{U} - 1)\Gamma(2d_\mathcal{U})}. \tag{3.2}$$

With the use of the spectral function $\rho(P^2)$ and requiring scale invariance, we can define the Feynman propagator. The propagator for the scalar unparticle is given by [2]

$$\Delta(p) = \frac{iA_{d_\mathcal{U}}}{2\sin(d_\mathcal{U}\pi)}(-p^2)^{d_\mathcal{U}-2}, \tag{3.3}$$

and similarly for the vector unparticle (with only the transverse mode),

$$\Delta^{\mu\nu}(p) = \frac{iA_{d_\mathcal{U}}}{2\sin(d_\mathcal{U}\pi)}(-p^2)^{d_\mathcal{U}-2}\left(g^{\mu\nu} - \frac{p^\mu p^\nu}{p^2}\right). \tag{3.4}$$

We could also consider the rigid conformal invariance as a symmetry of the hidden sector [26,27]. By requiring conformal invariance, the scalar unparticle propagator remains the same form, while the vector unparticle propagator is modified to

$$\Delta^{\mu\nu}(p) = \frac{iA_{d_\mathcal{U}}}{2\sin(d_\mathcal{U}\pi)}(-p^2)^{d_\mathcal{U}-2} \times \left(g^{\mu\nu} - \frac{2(d_\mathcal{U} - 2)}{d_\mathcal{U} - 1}\frac{p^\mu p^\nu}{p^2}\right). \tag{3.5}$$

In Ref. [27], the theoretical bound of the scaling dimension was obtained from the unitarity argument in this case. The scaling dimension for the scalar unparticle is constrained as $d_\mathcal{U} \geq 1$, while for the vector unparticle the bound is $d_\mathcal{U} \geq 3$. The vector unparticle interaction with the latter bound is very suppressed, and it would not cause a sizable deviation from the SM. In this paper, we will concentrate on the scale-invariant hidden sector, but we will also show some results for the conformal-invariant hidden sector with the scaling dimension $d_\mathcal{U} = 3.01$, satisfying the above-mentioned bound (see Table I).[3]

In the following we list operators composed of SM fields and derivatives which are relevant in our consideration. Relevant effective interactions of the scalar unparticle with the SM fields are given by

$$\frac{\lambda_{gg}}{\Lambda^{d_\mathcal{U}}}\,\mathrm{tr}(G^{\mu\nu}G_{\mu\nu})\mathcal{O}_\mathcal{U}, \tag{3.6}$$

for gluons, where λ_{gg} is a constant. For fermions we have (up to dimensionless coefficients)

$$\frac{1}{\Lambda^{d_\mathcal{U}}}\bar{Q}_L\gamma^\mu Q_L\partial_\mu\mathcal{O}_\mathcal{U}, \qquad \frac{1}{\Lambda^{d_\mathcal{U}}}\bar{U}_R\gamma^\mu U_R\partial_\mu\mathcal{O}_\mathcal{U}, \qquad \frac{1}{\Lambda^{d_\mathcal{U}}}\bar{D}_R\gamma^\mu D_R\partial_\mu\mathcal{O}_\mathcal{U}, \tag{3.7}$$

$$\frac{1}{\Lambda^{d_\mathcal{U}}}\bar{Q}_L\gamma^\mu D_\mu Q_L\mathcal{O}_\mathcal{U}, \qquad \frac{1}{\Lambda^{d_\mathcal{U}}}\bar{U}_R\gamma^\mu D_\mu U_R\mathcal{O}_\mathcal{U}, \qquad \frac{1}{\Lambda^{d_\mathcal{U}}}\bar{D}_R\gamma^\mu D_\mu D_R\mathcal{O}_\mathcal{U}, \tag{3.8}$$

[1] See [23] for the study of another spin basis, which has a larger spin correlation than the helicity basis at the LHC.

[2] The parton distribution function set of CTEQ6L [24] has been used in our calculations. The resultant spin asymmetry somewhat depends on the parton distribution functions used.

[3] In the analysis of the top spin correlations, the term proportional to $p^\mu p^\nu$ in the vector unparticle propagator is vanishing under the equation of motion for the initial (almost massless) light quark. Therefore, the difference between the scale-invariant and the conformal-invariant theories is just the bound for the scaling dimension.

TABLE I. Spin asymmetry $\mathcal{A}$ and the $t\bar{t}$ total cross section for the top-antitop events without the constraint on the invariant mass (second and third columns) and with the invariant mass cut (fourth and fifth columns) in the range $M_{t\bar{t}} \leq \Lambda$ GeV. The last row shows the SM results.

$d_{\mathcal{U}}$	$\mathcal{A}_{\rm SU}$	$\sigma_{\rm SU}$ (pb)	$\mathcal{A}_{\rm SU}^{\rm (cut)}$	$\sigma_{\rm SU}^{\rm (cut)}$ (pb)
1.01	0.335	502	0.333	501
1.10	0.325	495	0.324	494
$d_{\mathcal{U}}$	$\mathcal{A}_{\rm VU}$	$\sigma_{\rm VU}$ (pb)	$\mathcal{A}_{\rm VU}^{\rm (cut)}$	$\sigma_{\rm VU}^{\rm (cut)}$ (pb)
1.20	0.286	508	0.288	506
3.01	0.318	490	0.318	490
	$\mathcal{A}$	σ (pb)		
SM	0.319	489		

where Q_L is a left-handed quark, and $U_R(D_R)$ denotes a right-handed up (down)-type quark. The interactions with fermions can be simplified by utilizing the equation of motion for a fermion,

$$i\gamma^\mu \partial_\mu \psi = m_f \psi, \tag{3.9}$$

where m_f is a fermion mass. Consequently, (3.7) and (3.8) are summarized as

$$\frac{m_Q}{\Lambda^{d_{\mathcal{U}}}} \bar{Q}(a_Q^S + i\gamma^5 b_Q^S)Q, \tag{3.10}$$

where $Q = U$, D are mass eigenstates of quarks, and a_Q^S and b_Q^S are constants.

Possible terms interacting with the vector unparticle are

$$\frac{1}{\Lambda^{d_{\mathcal{U}}-1}} \bar{Q}_L \gamma^\mu Q_L (\mathcal{O}_{\mathcal{U}})_\mu, \qquad \frac{1}{\Lambda^{d_{\mathcal{U}}-1}} \bar{U}_R \gamma^\mu U_R (\mathcal{O}_{\mathcal{U}})_\mu,$$
$$\frac{1}{\Lambda^{d_{\mathcal{U}}-1}} \bar{D}_R \gamma^\mu D_R (\mathcal{O}_{\mathcal{U}})_\mu. \tag{3.11}$$

They are also simplified as

$$\frac{1}{\Lambda^{d_{\mathcal{U}}-1}} \bar{Q}\gamma^\mu (c_L^Q P_L + c_R^Q P_R) Q (\mathcal{O}_{\mathcal{U}})_\mu, \tag{3.12}$$

where c_L^Q and c_R^Q are coupling constants.

IV. AMPLITUDES

In this section we calculate the squared invariant amplitudes for $q\bar{q} \to t\bar{t}$ and $gg \to t\bar{t}$ processes. First we consider the effect of the scalar unparticle. In this case, we only consider the $gg \to t\bar{t}$ process for new contributions from the scalar unparticle, because the $q\bar{q} \to t\bar{t}$ process is proportional to light quark mass and hence negligible.

Since there is no interference between the QCD and the scalar unparticle mediated processes, the squared amplitude for the $gg \to t\bar{t}$ process is simply given by

$$|\mathcal{M}(gg \to t\bar{t})|^2 = |\mathcal{M}_{\rm QCD}(gg \to t\bar{t})|^2 + |\mathcal{M}_{\rm SU}(gg \to t\bar{t})|^2, \tag{4.1}$$

where $\mathcal{M}_{\rm QCD}$ is the amplitude of the QCD process and $\mathcal{M}_{\rm SU}$ is the contribution of the scalar unparticle. We calculate the helicity decomposition of the above amplitude with respect to the final top spin polarization. For the squared amplitude of the QCD process with the gg initial state, we have

$$|\mathcal{M}_{\rm QCD}(gg \to t_\uparrow \bar{t}_\uparrow)|^2 = |\mathcal{M}_{\rm QCD}(gg \to t_\downarrow \bar{t}_\downarrow)|^2 = \frac{g_s^4}{96} \mathcal{Y}(\beta_t, \cos\theta)(1-\beta_t^2) \times (1 + \beta_t^2 + \beta_t^2 \sin^4\theta), \tag{4.2}$$

$$|\mathcal{M}_{\rm QCD}(gg \to t_\uparrow \bar{t}_\downarrow)|^2 = |\mathcal{M}_{\rm QCD}(gg \to t_\downarrow \bar{t}_\uparrow)|^2 = \frac{g_s^4 \beta_t^2}{96} \mathcal{Y}(\beta_t, \cos\theta)\sin^2\theta(1+\cos^2\theta), \tag{4.3}$$

where g_s is the strong coupling constant, $\beta_t = \sqrt{1-4m_t^2/s}$, m_t is the top quark mass, $\sqrt{s}$ is the energy of colliding partons, and θ is the scattering angle between the incoming quark and the outgoing top quark. The form of $\mathcal{Y}(\beta_t, \theta)$ is defined by

$$\mathcal{Y}(\beta_t, \cos\theta) = \frac{7 + 9\beta_t^2 \cos^2\theta}{(1-\beta_t^2\cos^2\theta)^2}. \tag{4.4}$$

The squared helicity amplitude mediated by the scalar unparticle is written as

$$|\mathcal{M}_{\rm SU}(gg \to t_\gamma \bar{t}_\delta)|^2 = \left(\frac{1}{2}\right)^2 \left(\frac{1}{3^2-1}\right)^2 \frac{(3^2-1)3}{4} \times \sum_{\lambda_1,\lambda_2} |\mathcal{M}_{\rm SU}(\lambda_1, \lambda_2; \gamma, \delta)|^2, \tag{4.5}$$

where $\lambda_i (i = 1, 2) = \pm 1$ are the initial spins of gluons, and $\gamma = \pm (\delta = \pm)$ denotes spin up/down for the final state top (antitop) quark. The amplitude $\mathcal{M}_{\rm SU}(\lambda_1\lambda_2 \to t_\gamma \bar{t}_\delta)$ is the helicity decomposition of $\mathcal{M}_{\rm SU}(gg \to t_\gamma \bar{t}_\delta)$ with respect to the initial spins, given by

$$\mathcal{M}_{\rm SU}(\lambda_1, \lambda_2, \pm, \pm) = \pm \frac{A_{d_{\mathcal{U}}} \lambda_{gg} m_t e^{i\pi(d_{\mathcal{U}}-1/2)}}{\sin(d_{\mathcal{U}}\pi)\Lambda^{2d_{\mathcal{U}}}} s^{d_{\mathcal{U}}-1/2} \times \frac{1+\lambda_1\lambda_2}{2}(a_t^S \beta_t \mp i b_t^S), \tag{4.6}$$

$$\mathcal{M}_{\rm SU}(\lambda_1, \lambda_2, \pm, \mp) = 0. \tag{4.7}$$

For the $q\bar{q} \to t\bar{t}$ process, we have

$$|\mathcal{M}(q\bar{q} \to t\bar{t})|^2 = |\mathcal{M}_{\rm QCD}(q\bar{q} \to t\bar{t})|^2 + |\mathcal{M}_{\rm NC}(q\bar{q} \to t\bar{t})|^2, \tag{4.8}$$

where $\mathcal{M}_{\rm QCD}$ and $\mathcal{M}_{\rm NC}$ are the amplitudes of the QCD and the neutral current processes, respectively. The helicity decomposition of $\mathcal{M}_{\rm QCD}$ with respect to the final state is given by

$$|\mathcal{M}_{\rm QCD}(q\bar{q} \to t_\uparrow \bar{t}_\uparrow)|^2 = |\mathcal{M}_{\rm QCD}(q\bar{q} \to t_\downarrow \bar{t}_\downarrow)|^2 = \frac{g_s^4}{9}(1-\beta_t^2)\sin^2\theta, \tag{4.9}$$

$$|\mathcal{M}_{\rm QCD}(q\bar{q} \to t_\uparrow \bar{t}_\downarrow)|^2 = |\mathcal{M}_{\rm QCD}(q\bar{q} \to t_\downarrow \bar{t}_\uparrow)|^2 = \frac{g_s^4}{9}(1+\cos^2\theta). \tag{4.10}$$

The helicity amplitude of $\mathcal{M}_{\rm NC}$ is written as

$$|\mathcal{M}_{\rm NC}(q\bar{q} \to t_\gamma \bar{t}_\delta)|^2 = \left(\frac{1}{2}\right)^2 \sum_{\alpha,\beta} |\mathcal{M}_{\rm NC}(\alpha,\beta;\gamma,\delta)|^2, \tag{4.11}$$

where $\mathcal{M}_{\rm NC}(\alpha,\beta;\gamma,\delta)$ are the helicity amplitudes and the symbols $\alpha(\gamma)$ and $\beta(\delta)$ denote initial (final) spin states for quarks and antiquarks, respectively. They are described by (the color factor is suppressed)

$$\mathcal{M}_{\rm NC}(+,-;\pm,\pm) = \mp s\sqrt{1-\beta_t^2}\sin\theta\left[\frac{(eQ^f)(eQ^t)}{s} + \frac{g_R^f}{2}\frac{g_L^t+g_R^t}{s-M_Z^2+iM_Z\Gamma_Z}\right], \tag{4.12}$$

$$\mathcal{M}_{\rm NC}(-,+;\pm,\pm) = \mp s\sqrt{1-\beta_t^2}\sin\theta\left[\frac{(eQ^f)(eQ^t)}{s} + \frac{g_L^f}{2}\frac{g_L^t+g_R^t}{s-M_Z^2+iM_Z\Gamma_Z}\right], \tag{4.13}$$

$$\mathcal{M}_{\rm NC}(+,-;+,-) = -s(1+\cos\theta)\left[\frac{(eQ^f)(eQ^t)}{s} + \frac{g_R^f}{2}\frac{(1-\beta_t)g_L^t+(1+\beta_t)g_R^t}{s-M_Z^2+iM_Z\Gamma_Z}\right], \tag{4.14}$$

$$\mathcal{M}_{\rm NC}(+,-;-,+) = s(1-\cos\theta)\left[\frac{(eQ^f)(eQ^t)}{s} + \frac{g_R^f}{2}\frac{(1+\beta_t)g_L^t+(1-\beta_t)g_R^t}{s-M_Z^2+iM_Z\Gamma_Z}\right], \tag{4.15}$$

$$\mathcal{M}_{\rm NC}(-,+;+,-) = s(1-\cos\theta)\left[\frac{(eQ^f)(eQ^t)}{s} + \frac{g_L^f}{2}\frac{(1-\beta_t)g_L^t+(1+\beta_t)g_R^t}{s-M_Z^2+iM_Z\Gamma_Z}\right], \tag{4.16}$$

$$\mathcal{M}_{\rm NC}(-,+;-,+) = -s(1+\cos\theta)\left[\frac{(eQ^f)(eQ^t)}{s} + \frac{g_L^f}{2}\frac{(1+\beta_t)g_L^t+(1-\beta_t)g_R^t}{s-M_Z^2+iM_Z\Gamma_Z}\right], \tag{4.17}$$

with the decay widths of the Z boson, Γ_Z, given by

$$\Gamma_Z = \Gamma(Z \to f\bar{f}) = \frac{M_Z}{96\pi}\sum_f \beta^f\{(3+(\beta^f)^2)((g_L^f)^2+(g_R^f)^2) + 6(1-(\beta^f)^2)g_L^f g_R^f\}. \tag{4.18}$$

Here M_Z is the mass of the Z boson and $\beta^f = \sqrt{1-4m_f^2/M_Z^2}$. Couplings, charges, and decay widths Γ_Z are explicitly given in the Appendix.

Next we consider the case for the vector unparticle, which contributes to the quark annihilation process $q\bar{q} \to t\bar{t}$ in the s, t, and u channels, in addition to the standard model processes. In our analysis, we assume no flavor-violating processes, and therefore we only consider the vector unparticle exchange in the s-channel process. The total amplitude for the quark annihilation process is given by

$$\mathcal{M}(q\bar{q} \to t\bar{t}) = \mathcal{M}_{\rm NC}(q\bar{q} \to t\bar{t}) + \mathcal{M}_{\rm QCD}(q\bar{q} \to t\bar{t}) + \mathcal{M}_{\rm VU}(q\bar{q} \to t\bar{t}), \tag{4.19}$$

where $\mathcal{M}_{\rm NC}$ is the neutral current process, $\mathcal{M}_{\rm QCD}$ is the QCD process given in (4.9) and (4.10), and $\mathcal{M}_{\rm VU}$ is the contribution of the vector unparticle. Since there is no interference between the QCD process and other processes, the squared amplitude is written as

$$|\mathcal{M}(q\bar{q} \to t\bar{t})|^2 = |(\mathcal{M}_{\rm NC}+\mathcal{M}_{\rm VU})(q\bar{q} \to t\bar{t})|^2 + |\mathcal{M}_{\rm QCD}(q\bar{q} \to t\bar{t})|^2. \tag{4.20}$$

The helicity amplitude of the neutral current process and the vector unparticle mediated process is described by

$$|(\mathcal{M}_{\rm NC}+\mathcal{M}_{\rm VU})(q\bar{q} \to t_\gamma \bar{t}_\delta)|^2 = \left(\frac{1}{2}\right)^2 \sum_{\alpha,\beta}(|\mathcal{M}_{\rm NC}(\alpha,\beta;\gamma,\delta)|^2 + |\mathcal{M}_{\rm VU}(\alpha,\beta;\gamma,\delta)|^2 + (\mathcal{M}_{\rm NC}\mathcal{M}_{\rm VU}^*(\alpha,\beta;\gamma,\delta) + \text{H.c.})), \tag{4.21}$$

where $\mathcal{M}_{\rm VU}(\alpha, \beta; \gamma, \delta)$ are the decompositions of the helicity amplitudes $\mathcal{M}_{\rm VU}(q\bar{q} \to t_\gamma \bar{t}_\delta)$ with respect to the initial spin.

The helicity amplitudes mediated by the vector unparticle $\mathcal{M}_{\rm VU}(\alpha, \beta; \gamma, \delta)$ are given by

$$\mathcal{M}_{\rm VU}(+, -; \pm, \pm) = \pm s^{d_\mathcal{U}-1}\sqrt{1-\beta_t^2}\sin\theta \frac{A_{d_\mathcal{U}} e^{i\pi(d_\mathcal{U}-2)}}{2\sin(d_\mathcal{U}\pi)\Lambda^{2(d_\mathcal{U}-1)}} \frac{c_R^Q}{2}(c_L^t + c_R^t), \tag{4.22}$$

$$\mathcal{M}_{\rm VU}(-, +; \pm, \pm) = \pm s^{d_\mathcal{U}-1}\sqrt{1-\beta_t^2}\sin\theta \frac{A_{d_\mathcal{U}} e^{i\pi(d_\mathcal{U}-2)}}{2\sin(d_\mathcal{U}\pi)\Lambda^{2(d_\mathcal{U}-1)}} \frac{c_L^Q}{2}(c_L^t + c_R^t), \tag{4.23}$$

$$\mathcal{M}_{\rm VU}(+, -; \pm, \mp) = s^{d_\mathcal{U}-1}(\cos\theta \pm 1) \frac{A_{d_\mathcal{U}} e^{i\pi(d_\mathcal{U}-2)}}{2\sin(d_\mathcal{U}\pi)\Lambda^{2(d_\mathcal{U}-1)}} \frac{c_R^Q}{2}(c_L^t + c_R^t \mp \beta_t(c_L^t - c_R^t)), \tag{4.24}$$

$$\mathcal{M}_{\rm VU}(-, +; \pm, \mp) = s^{d_\mathcal{U}-1}(\cos\theta \mp 1) \frac{A_{d_\mathcal{U}} e^{i\pi(d_\mathcal{U}-2)}}{2\sin(d_\mathcal{U}\pi)\Lambda^{2(d_\mathcal{U}-1)}} \frac{c_L^Q}{2}(c_L^t + c_R^t \mp \beta_t(c_L^t - c_R^t)), \tag{4.25}$$

where $c_L^t(c_R^t)$ is the coupling constant $c_L^Q(c_R^Q)$ in (3.12) with $Q = t$.

V. NUMERICAL ANALYSIS

Here we show various numerical results and demonstrate interesting properties of measurable quantities. In our analysis we use the parton distribution function of CTEQ6L [24] with the factorization scale $Q = m_t = 175$ GeV and $\alpha_s(Q) = 0.1074$. In the whole analysis, the center-of-mass energy of the colliding protons, $E_{\rm CMS}$, is taken to be 1.96 TeV at the Tevatron and 14 TeV at the LHC. For simplicity, we fix the model parameters as follows: $\lambda_{gg} = 1$ in (3.6), $a_Q^S = b_Q^S = c_L^Q = c_R^Q = 1$ in (3.10) and (3.12), and $\Lambda = 1$ TeV.

As can be seen from the formulas of the squared amplitudes (4.6), (4.22), (4.23), (4.24), and (4.25), the cross sections through the unparticle exchange processes grow or slowly decrease compared to the SM cross sections, according to the colliding partons center-of-mass energy. When the cross section grows as a power of the center-of-mass energy, the unitarity will be violated at high energies. This behavior is shown, for instance, in Figs. 1 and 2, where the cross sections of the top-antitop pair production through $q\bar{q} \to t\bar{t}$ and $gg \to t\bar{t}$ at the parton level, respectively, are depicted as a function of the parton center-of-mass energy $M_{t\bar{t}}$. In order to make our analysis conservative, we only take into account the contributions from unparticle exchange processes for the center-of-mass en-

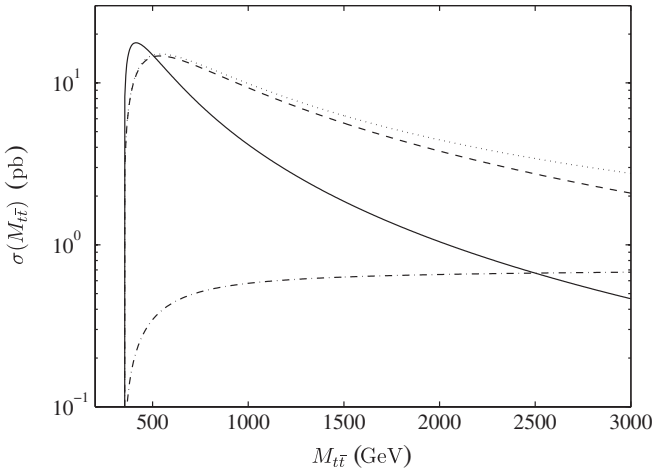

FIG. 1. The dependence of the cross section of the top-antitop quark pair production by quark pair annihilation and gluon fusion on the center-of-mass energy of colliding partons $M_{t\bar{t}}$ with $d_\mathcal{U} = 1.01$ and $\Lambda = 1$ TeV. The solid and dashed lines correspond to the results of up-quark annihilation and gluon fusion for the SM, respectively. The dotted and dash-dotted lines correspond to the results of the SM(gluon fusion) + the scalar unparticle processes, and only the scalar unparticle contribution.

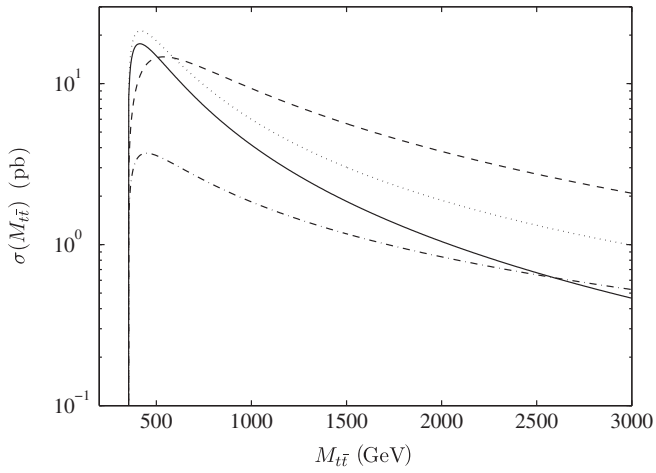

FIG. 2. The dependence of the cross section of the top-antitop quark pair production by quark pair annihilation and gluon fusion on the center-of-mass energy of colliding partons $M_{t\bar{t}}$ with $d_\mathcal{U} = 1.01$ and $\Lambda = 1$ TeV. The solid and dashed lines correspond to the results of the up-quark annihilation and gluon fusion for the SM, respectively. The dotted and dash-dotted lines correspond to the results of the SM(up-quark annihilation) + vector unparticle processes, and only the vector unparticle contribution.

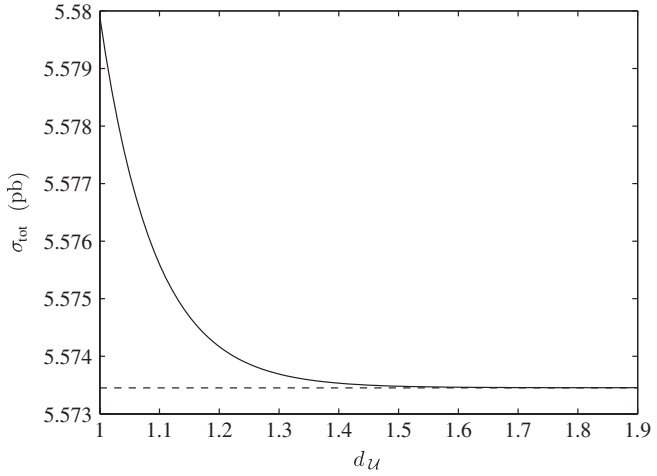

FIG. 3. The total cross section of the top-antitop quark pair production as a function of $d_{\mathcal{U}}$ at Tevatron with $\sqrt{s} = 1.96$ TeV and $\Lambda = 1$ TeV. The solid curve shows the value of the SM + scalar unparticle, while the dashed line shows the SM value.

ergy of colliding partons lower than Λ, namely, $\sqrt{s} = M_{t\bar{t}} \leq \Lambda$.

The scaling dimension of the unparticle $d_{\mathcal{U}}$ is a unique free parameter in our analysis. Since the Tevatron results for the total cross section of top-antitop production are consistent with the SM prediction [28], we can obtain the lower bounds for $d_{\mathcal{U}}$ from the Tevatron results. In Figs. 3 and 4, we present the dependence of the total cross section on $d_{\mathcal{U}}$ in the case of the scalar and the vector unparticles. The solid line corresponds to the model with unparticles, while the dashed line corresponds to the SM value. We find the SM cross section for the top-antitop pair production at

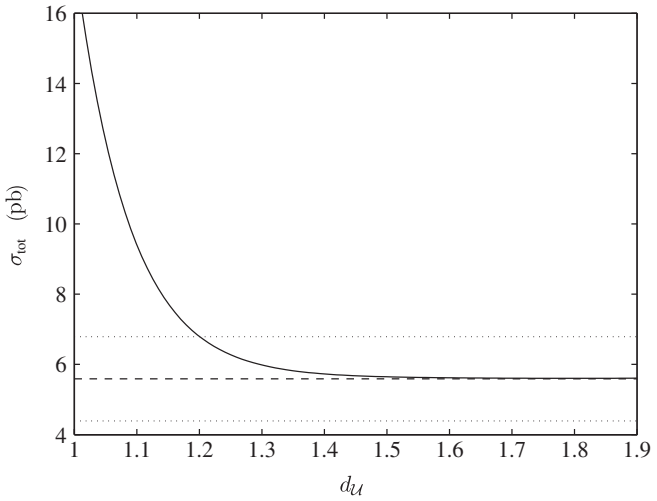

FIG. 4. The total cross section of the top-antitop quark pair production as a function of $d_{\mathcal{U}}$ at Tevatron with $\sqrt{s} = 1.96$ TeV and $\Lambda = 1$ TeV. The solid curve shows the contribution of the vector unparticle to the total cross section. The dashed line corresponds to the SM value, and the dotted lines correspond to the estimated errors from the Tevatron measurement.

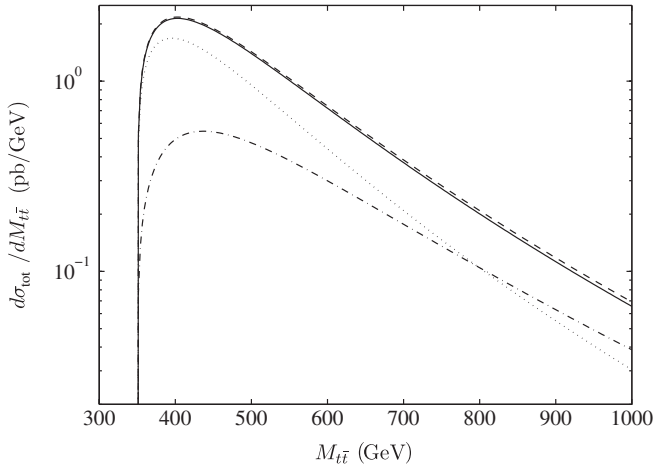

FIG. 5. Differential cross section (5.1) as a function of the top-antitop invariant mass $M_{t\bar{t}}$ for the SM + scalar unparticle processes with $d_{\mathcal{U}} = 1.01$ and $\Lambda = 1$ TeV. The solid line depicts the result of the SM, and the dashed line depicts the result of the SM + scalar unparticle. The breakdown of the latter into the like-spin (dotted) and the unlike-spin (dash-dotted) pair productions is also shown.

LO to be $\sim$5.57 pb, while in the next-to-next-to-LO (NNLO) analysis the SM prediction is found to be $6.7^{+0.7}_{-0.9}$ pb [29]. Scaling our results to the NNLO value, we estimate the error of the Tevatron measurement as ± 1.2 pb and apply this error bar to obtain the lower bound on $d_{\mathcal{U}}$ (see Fig. 4). From the plots, we find that there is no bound on $d_{\mathcal{U}}(\geq 1)$ for the scalar unparticle, while $d_{\mathcal{U}} \geq 1.2$ for the vector unparticle.

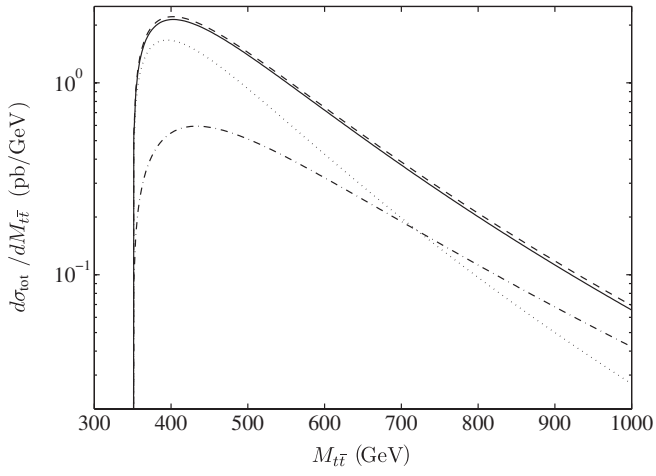

FIG. 6. Differential cross section (5.1) as a function of the top-antitop invariant mass $M_{t\bar{t}}$ for the SM + vector unparticle processes with $d_{\mathcal{U}} = 1.20$ and $\Lambda = 1$ TeV. The solid line depicts the result of the SM, and the dashed line depicts the result of the SM + vector unparticle. The breakdown of the latter into the like-spin (dotted line) and the unlike-spin (dash-dotted line) pair productions is also shown.

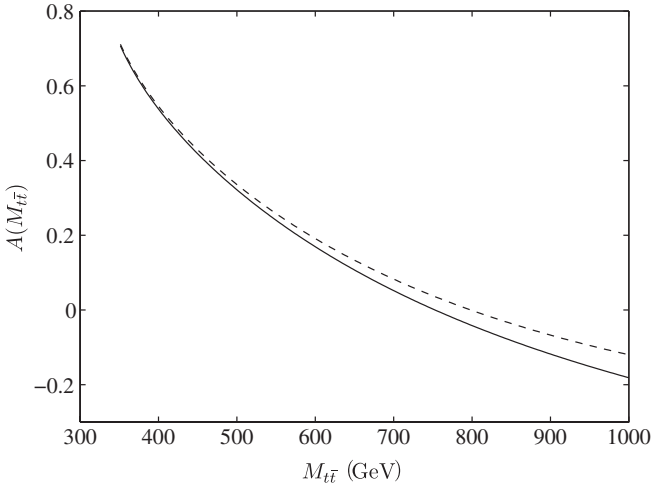

FIG. 7. Spin asymmetry $\mathcal{A}$ as a function of the top-antitop invariant mass $M_{t\bar{t}}$ with $d_{\mathcal{U}} = 1.01$ and $\Lambda = 1$ TeV. The solid line corresponds to the SM, while the dashed line corresponds to the result of the SM + scalar unparticle.

With the lower bound on $d_{\mathcal{U}}$ from the Tevatron experiment, we now consider the unparticle effects on the top-antitop production process at the LHC. The dependence of the cross section on the top-antitop invariant mass $M_{t\bar{t}}$ is given by

$$\frac{d\sigma_{\text{tot}}(pp \to t\bar{t})}{d\sqrt{s}} = \sum_{a,b} \int_{-1}^{1} d\cos\theta \int_{\frac{s}{E^2_{\text{CMS}}}}^{1} dx_1 \frac{2\sqrt{s}}{x_1 E^2_{\text{CMS}}} \times f_a(x_1, Q^2) f_b\left(\frac{s}{x_1 E^2_{\text{CMS}}}, Q^2\right) \frac{d\sigma(t\bar{t})}{d\cos\theta}. \tag{5.1}$$

Figures 5 and 6 show the same dependence for the case of the scalar and the vector unparticles. Here, the decomposition of the total cross section into the like $(t_\uparrow \bar{t}_\uparrow + t_\downarrow \bar{t}_\downarrow)$ and unlike $(t_\uparrow \bar{t}_\downarrow + t_\downarrow \bar{t}_\uparrow)$ top-antitop spin pairs is also shown.

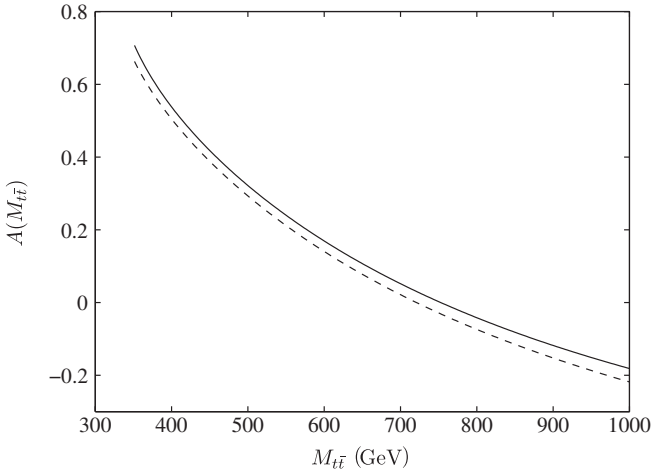

FIG. 8. Spin asymmetry $\mathcal{A}$ as a function of the top-antitop invariant mass $M_{t\bar{t}}$ with $d_{\mathcal{U}} = 1.20$ and $\Lambda = 1$ TeV. The solid line corresponds to the SM, while the dashed line corresponds to the result of the SM + vector unparticle.

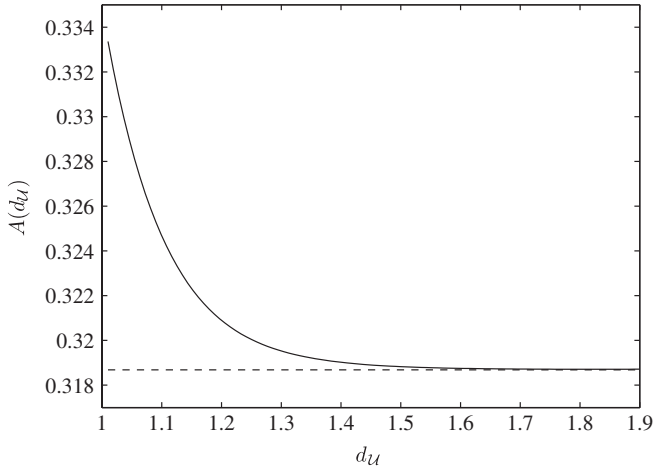

FIG. 9. Spin asymmetry $\mathcal{A}$ as a function of $d_{\mathcal{U}}$ for the case of the scalar unparticle with $\Lambda = 1$ TeV.

Now we show the results for the spin asymmetry $\mathcal{A}$ as a function of the top-antitop invariant mass $M_{t\bar{t}}$. The plot for the case of the scalar unparticle is shown in Fig. 7 and for the vector unparticle in Fig. 8. The dependence of $\mathcal{A}$ on the value of $d_{\mathcal{U}}$, after integration with respect to $M_{t\bar{t}}$ in the range $2m_t \leq M_{t\bar{t}} \leq E_{\text{CMS}}$, is depicted in Figs. 9 and 10. The existence of the scalar unparticle increases the value of $\mathcal{A}$, while the existence of the vector unparticle decreases the expected spin asymmetry. Deviation from the SM becomes larger as the center-of-mass energy becomes larger and $d_{\mathcal{U}}$ becomes smaller. In Figs. 11 and 12, the results for the spin asymmetry $\mathcal{A}$ as a function of the effective cutoff scale Λ are depicted. Again, one can see that the scalar (vector) unparticle gives rise to positive (negative) contributions to $\mathcal{A}$.

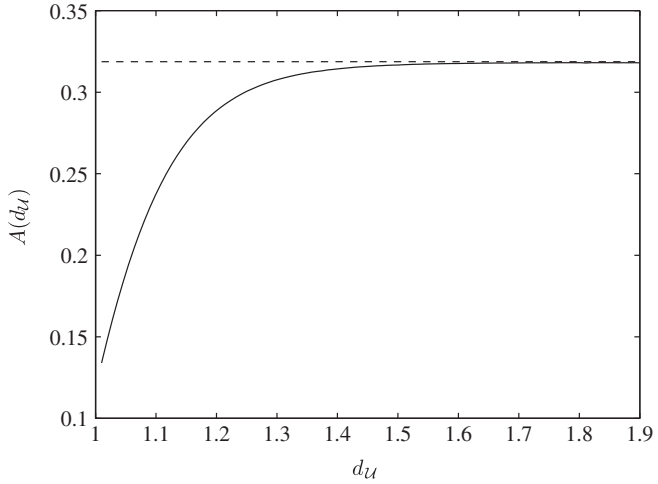

FIG. 10. Spin asymmetry $\mathcal{A}$ as a function of $d_{\mathcal{U}}$ for the case of the vector unparticle with $\Lambda = 1$ TeV.

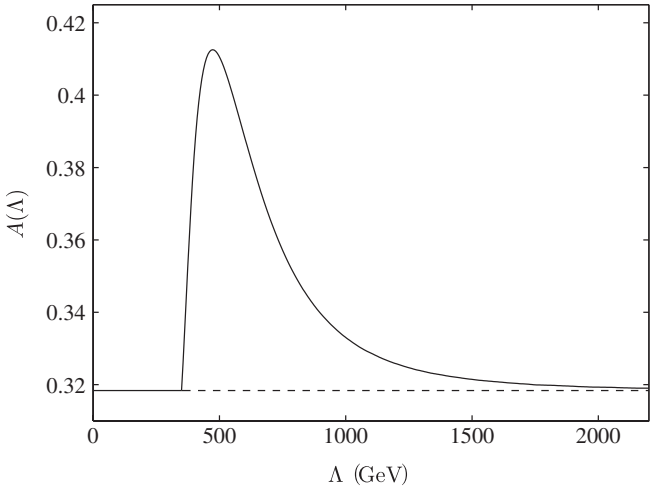

FIG. 11. Spin asymmetry $\mathcal{A}$ as a function of Λ for the case of the scalar unparticle with $d_{\mathcal{U}} = 1.01$.

Table I presents values of the spin asymmetry $\mathcal{A}$ and the $t\bar{t}$ total cross section for selected values of $d_{\mathcal{U}}$. Here, $\mathcal{A}^{(\mathrm{cut})}$ and $\sigma^{(\mathrm{cut})}$ denote the results when we take into account the unparticle contributions only for the range $\sqrt{s} = M_{t\bar{t}} \leq \Lambda$. For the spin asymmetry $\mathcal{A}$, we see a deviation of $\sim$5% for the allowed value of $d_{\mathcal{U}} = 1.01$ for the model with the scalar unparticle, and $\sim$10% for the allowed value of $d_{\mathcal{U}} = 1.20$ for the model with the vector unparticle. Note that for a fixed $d_{\mathcal{U}}$, the deviation of the spin asymmetry from the SM one is always bigger than the deviation of the total cross sections. With the estimated precision of the measurement around 6% [25], the size of the deviation from the SM for the vector unparticle could be sufficient for the observation in the data from the first year of the low luminosity LHC run (with integral luminosity $\mathcal{L} = 10\ \mathrm{fb}^{-1}$). For higher values of $d_{\mathcal{U}}$, the interactions between the unparticles and the SM are suppressed, and thus the deviation is very small. In particular, the vector unparticle with rigid conformal invariance, where $d_{\mathcal{U}} \geq 3$, does not give rise to large deviations.

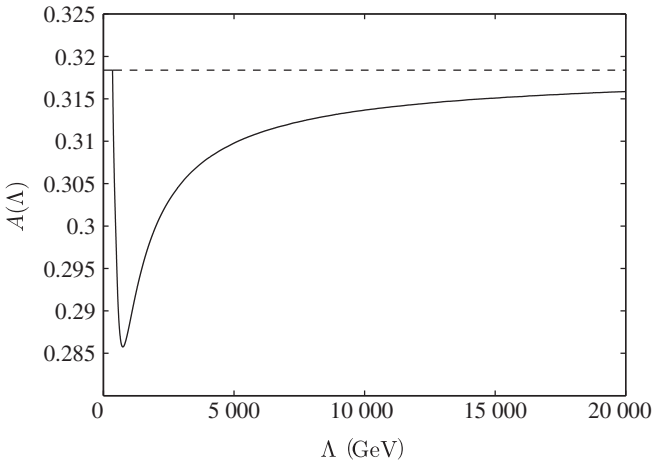

FIG. 12. Spin asymmetry $\mathcal{A}$ as a function of Λ for the case of the vector unparticle with $d_{\mathcal{U}} = 1.20$.

VI. CONCLUSION

We have studied the top-antitop pair production and the top spin correlations with the scalar and the vector unparticles at the LHC. In addition to the SM processes, there is a new contribution to the top-antitop pair production process mediated by unparticles in the s channel. We have computed the corresponding density matrix for the top-antitop pair production including the contributions from the scalar unparticle and the vector unparticle exchanges. The scalar unparticle contributes to the like-spin pair production amplitude through the gluon fusion processes, while the vector unparticle mainly contributes to the unlike-spin pair through the quark annihilation process.

We have shown various numerical results for the production cross sections and the top spin correlations with certain values of the scaling dimension $d_{\mathcal{U}}$ and the cutoff Λ. We have found a sizable deviation of the top-antitop pair production cross sections and the top spin correlations from those in the SM for the scalar and vector unparticle exchange processes with lower values of the scaling dimensions $d_{\mathcal{U}}$. In particular, for the spin correlation, we have found deviations of about 5% and 10% of the spin asymmetry from the SM one for the scalar unparticle and the vector unparticle, respectively. In Ref. [25], it is shown that the spin asymmetry of the top-antitop pairs in the SM will be measured with a precision of 6% after one year at LHC at low luminosity, 10 fb^{-1}. Thus, the deviation of the top spin symmetry by the vector unparticle effects can be measurable. However, note that it is a very rough estimation since the sensitivity of the ATLAS experiment on the spin correlation published in [25] was estimated selecting low energetic top quarks with $M_{t\bar{t}} < 550$ GeV. In order to estimate the sensitivity more accurately with a high $M_{t\bar{t}}$ region for our case, we need elaborate Monte Carlo simulations, including the detector response. We leave this interesting subject for future study.

ACKNOWLEDGMENTS

The authors would like to thank Santosh Kumar Rai and Vladislav Šimák for illuminating discussions. The work of M. A. is supported by the Science Research Center Program of the Korea Science and Engineering Foundation through the Center for Quantum Spacetime (CQUeST) of Sogang University with Grant No. R11-2005-021. M. A. would also like to thank Czech Technical University in Prague and the Theory Division of KEK for their hospitality during his visit. The work of N. O. is supported in part by the Grant-in-Aid for Scientific Research from the Ministry of Education, Science and Culture of Japan (No. 18740170). The work of K. S. is

supported by the Research Program MSM6840770029 and by the project International Cooperation ATLAS-CERN of the Ministry of Education, Youth and Sports of the Czech Republic.

APPENDIX: COUPLINGS AND DECAY WIDTHS

The couplings for the SM Z boson are

$$g^{\nu}_{L,1} = \frac{e}{\cos\theta_W \sin\theta_W}\frac{1}{2}, \qquad g^{\nu}_{R,1} = 0, \tag{A1}$$

$$\begin{aligned} g^{l}_{L,1} &= \frac{e}{\cos\theta_W \sin\theta_W}\left(-\frac{1}{2} - \sin^2\theta_W(-1)\right), \\ g^{l}_{R,1} &= -e(-1)\tan\theta_W, \end{aligned} \tag{A2}$$

$$\begin{aligned} g^{u}_{L,1} &= \frac{e}{\cos\theta_W \sin\theta_W}\left(\frac{1}{2} - \sin^2\theta_W\frac{2}{3}\right), \\ g^{u}_{R,1} &= -e\frac{2}{3}\tan\theta_W, \end{aligned} \tag{A3}$$

$$\begin{aligned} g^{d}_{L,1} &= \frac{e}{\cos\theta_W \sin\theta_W}\left(-\frac{1}{2} - \sin^2\theta_W\left(-\frac{1}{3}\right)\right), \\ g^{d}_{R,1} &= -e\left(-\frac{1}{3}\right)\tan\theta_W. \end{aligned} \tag{A4}$$

The decay widths of the Z boson are

$$\Gamma(Z \to \nu\bar{\nu}) = \frac{M_Z}{24\pi}((g^{\nu}_L)^2 + (g^{\nu}_R)^2), \tag{A5}$$

$$\Gamma(Z \to l\bar{l}) = \frac{M_Z}{24\pi}((g^{l}_L)^2 + (g^{l}_R)^2), \tag{A6}$$

$$\Gamma(Z \to u\bar{u}) = \frac{M_Z}{24\pi}3((g^{u}_L)^2 + (g^{u}_R)^2), \tag{A7}$$

$$\Gamma(Z \to d\bar{d}) = \frac{M_Z}{24\pi}3((g^{d}_L)^2 + (g^{d}_R)^2). \tag{A8}$$

[1] H. Georgi, Phys. Rev. Lett. **98**, 221601 (2007).
[2] H. Georgi, Phys. Lett. B **650**, 275 (2007).
[3] T. Banks and A. Zaks, Nucl. Phys. **B196**, 189 (1982).
[4] K. Cheung, W. Y. Keung, and T. C. Yuan, Phys. Rev. Lett. **99**, 051803 (2007).
[5] F. Abe *et al.* (CDF Collaboration), Phys. Rev. Lett. **74**, 2626 (1995).
[6] I. I. Y. Bigi, Y. L. Dokshitzer, V. A. Khoze, J. H. Kuhn, and P. M. Zerwas, Phys. Lett. B **181**, 157 (1986).
[7] T. Stelzer and S. Willenbrock, Phys. Lett. B **374**, 169 (1996); A. Brandenburg, Phys. Lett. B **388**, 626 (1996); D. Chang, S. C. Lee, and A. Sumarokov, Phys. Rev. Lett. **77**, 1218 (1996).
[8] G. Mahlon and S. J. Parke, Phys. Rev. D **53**, 4886 (1996); Phys. Lett. B **411**, 173 (1997).
[9] W. Bernreuther, A. Brandenburg, Z. G. Si, and P. Uwer, Phys. Rev. Lett. **87**, 242002 (2001); Nucl. Phys. **B690**, 81 (2004).
[10] K. Y. Lee, H. S. Song, J. H. Song, and C. Yu, Phys. Rev. D **60**, 093002 (1999); K. Y. Lee, S. C. Park, H. S. Song, and C. Yu, Phys. Rev. D **63**, 094010 (2001); C. X. Yue, L. Wang, L. N. Wang, and Y. M. Zhang, Chin. Phys. Lett. **23**, 2379 (2006).
[11] K. Y. Lee, S. C. Park, H. S. Song, J. H. Song, and C. Yu, Phys. Rev. D **61**, 074005 (2000).
[12] M. Arai, N. Okada, K. Smolek, and V. Šimák, Phys. Rev. D **70**, 115015 (2004).
[13] M. Arai, N. Okada, K. Smolek, and V. Šimák, Phys. Rev. D **75**, 095008 (2007).
[14] M. Arai, N. Okada, K. Smolek, and V. Šimák, Acta Phys. Pol. B **40**, 93 (2009).
[15] R. Frederix and F. Maltoni, J. High Energy Phys. 01 (2009) 047.
[16] D. Choudhury and D. K. Ghosh, Int. J. Mod. Phys. A **23**, 2579 (2008).
[17] A. T. Alan and N. K. Pak, Europhys. Lett. **84**, 11001 (2008).
[18] H. F. Li, H. L. Li, Z. G. Si, and Z. J. Yang, arXiv:0802.0236.
[19] B. Sahin, arXiv:0802.1937.
[20] I. Sahin, Eur. Phys. J. C **60**, 431 (2009).
[21] A. Czarnecki, M. Jezabek, and J. H. Kühn, Nucl. Phys. **B351**, 70 (1991).
[22] W. Bernreuther, O. Nachtmann, P. Overmann, and T. Schröder, Nucl. Phys. **B388**, 53 (1992); **B406**, 516(E) (1993); A. Brandenburg and J. P. Ma, Phys. Lett. B **298**, 211 (1993).
[23] P. Uwer, Phys. Lett. B **609**, 271 (2005).
[24] J. Pumplin, D. R. Stump, J. Huston, H. L. Lai, P. Nadolsky, and W. K. Tung, J. High Energy Phys. 07 (2002) 012.
[25] F. Hubaut, E. Monnier, P. Pralavorio, V. Šimák, and K. Smolek, Eur. Phys. J. C **44**, 13 (2005).
[26] G. Mack and K. Symanzik, Commun. Math. Phys. **27**, 247 (1972).
[27] B. Grinstein, K. Intriligator, and I. Z. Rothstein, Phys. Lett. B **662**, 367 (2008).
[28] CDF Collaboration, CDF Report No. 9399.
[29] M. Cacciari *et al.*, J. High Energy Phys. 04 (2004) 068.